[CANCER RESEARCH 64, 8994–9001, December 15, 2004]

Conditional ROCK Activation *In vivo* Induces Tumor Cell Dissemination and Angiogenesis

Daniel R. Croft,[1] Erik Sahai,[2] Georgia Mavria,[3] Shuixing Li,[1] Jeff Tsai,[4] William M. F. Lee,[4] Christopher J. Marshall,[3] and Michael F. Olson[1]

[1]Abramson Family Cancer Research Institute, University of Pennsylvania School of Medicine, Philadelphia, Pennsylvania; [2]Cancer Research UK London Research Institute, London, United Kingdom; [3]The Institute of Cancer Research, London, United Kingdom; and [4]Department of Medicine and Cancer Center, University of Pennsylvania Medical Center, Philadelphia, Pennsylvania

ABSTRACT

Progression of tumors to invasive and metastatic forms requires that tumor cells undergo dramatic morphologic changes, a process regulated by Rho GTPases. Elevated expression of RhoA and RhoC, as well as the Rho effector proteins ROCK I and ROCK II, are commonly observed in human cancers and are often associated with more invasive and metastatic phenotypes. To examine how ROCK contributes to the progression of solid tumors, we established a conditionally activated form of ROCK II by fusing the kinase domain to the estrogen receptor hormone-binding domain (ROCK:ER). ROCK:ER-expressing colon carcinoma cells grown as tumors in immunocompromised nude mice organized into discrete clusters surrounding blood vessels. However, ROCK:ER activation resulted in the aggressive dissemination of tumor cells into the surrounding stroma, indicating that increased ROCK signaling is sufficient to promote invasion from solid tumors. In addition, tumors in which ROCK:ER was activated were more highly vascularized, indicating that ROCK contributes to tumor angiogenesis. ROCK:ER activation resulted in changes to epithelial morphology and organization that facilitated motility *in vitro*, likely by inducing the redistribution of proteins such as ezrin, as well as adherens junction and extracellular matrix-binding proteins. These results suggest that ROCK inhibitors would be useful antimetastatic and antiangiogenic chemotherapeutic agents in tumors associated with elevated RhoA, RhoC, ROCK I, or ROCK II expression.

INTRODUCTION

The process of metastasis involves a restructuring of the cytoskeleton as well as cell–cell and cell–matrix adhesions allowing cells to break away from the tumor mass, invade local tissue, and ultimately spread throughout the body. These effects on cell morphology and adhesion are regulated by members of the Rho GTPase family (1). Although Rho GTPases have been implicated in human cancer (2), mutation does not appear to be a mode of Rho activation, in contrast to Ras proteins (mutated versions of Ras proteins have been detected in tumors). However, RhoA and RhoC protein levels are significantly elevated in a variety of tumors, especially during progression to more invasive and metastatic forms (2–12). Moreover, microarray analysis of metastasis-inducing genes identified RhoC in an experimental mouse melanoma model (13). In addition to elevated RhoA and RhoC, increased levels of the Rho effector proteins ROCK I and/or ROCK II were observed in esophageal squamous cell carcinoma (14) and in testicular germ cell (3), pancreatic (15), and bladder tumors (6). ROCK II expression was also found to be higher in a metastatic variant of a nonmetastatic rat mammary adenocarcinoma cell line when grown as subcutaneous tumors (16). Thus, elevated Rho and ROCK expression are associated with tumorigenesis, particularly during the progression to invasive and metastatic phenotypes.

Rho family GTPases are key regulators of many different biological processes including cell motility, and Cdc42, Rac1, and RhoA are the most extensively studied family members (1, 17). When bound to GTP, these proteins recruit effector proteins that influence the architecture of the actin cytoskeleton. RhoA and RhoC activate the serine/threonine kinases ROCK I (also called ROKβ) and ROCK II (ROKα or Rho kinase; ref. 18). ROCK activation promotes the stabilization of filamentous actin (F-actin), phosphorylation of regulatory myosin light chains (MLCs), increased myosin ATPase activity, and the coupling of actin-myosin filaments to the plasma membrane, leading to increased actin-myosin force generation and contractility. In fibroblasts grown in tissue culture, RhoA signals through ROCK I and ROCK II to promote the formation of contractile actin-myosin bundles commonly known as stress fibers and focal adhesions leading to increased substrate adherence (19, 20). However, genetic experiments in *Drosophila* revealed that elevated Rho signaling in epithelial cells resulted in a loss of epithelial characteristics and increased invasive migratory behavior (21). These results indicate that the consequences of Rho and ROCK signaling likely depend on cell type and cellular context.

Given the elevated RhoA, RhoC, ROCK I, and ROCK II expression associated with tumor progression to more advanced stages, it has been suggested that Rho and ROCK signaling contribute to the morphologic changes and metastatic behavior of some tumor cells. Tumor cell movement through three-dimensional matrices occurs via two modes, either an elongated protease-dependent ROCK inhibitor-insensitive mechanism or a rounded protease-independent ROCK inhibitor-sensitive mechanism (22). *In vivo* studies have also shown that ROCK inhibition reduced the invasiveness of several tumor cell lines (23–28). However, the design of these *in vivo* studies does not necessarily indicate that the tumor cell was the critical inhibitor target; ROCK inhibition may largely block tumor cell invasion by enhancing the barrier function of host cell layers (29, 30).

To study the effects of ROCK signaling on epithelial tumor cell behavior *in vitro* and *in vivo*, we created a conditionally activated form of ROCK II. Retroviral vectors encoding the kinase domain fused to the estrogen receptor hormone-binding domain were constructed, thereby generating ROCK:ER. As a control, mutant ROCK II in which a lysine in the ATP-binding pocket was changed to glycine (K121G) was used to generate kinase-dead KD:ER. HCT116 and LS174T human colon carcinoma cell lines expressing ROCK:ER or KD:ER were established, and we examined *in vitro* ROCK activity after the addition of 4-hydroxytamoxifen (4-HT). Treatment of ROCK:ER-expressing cells with 4-HT resulted in increased kinase activity, both in tissue culture and in tumors grown in immunocompromised mice. To determine the effects of ROCK activation on

Received 6/10/04; revised 9/20/04; accepted 10/22/04.

Grant support: American Cancer Society RSG-04-078-01-TBE, National Cancer Institute grant RO1 CA030721-01A1, National Institute of Diabetes and Digestive and Kidney Diseases Center grant P30-DK50306, American Cancer Society Institutional Research Grant, University of Pennsylvania Cancer Center, University of Pennsylvania Cancer Center Core Grant Pilot Project Program, Thomas B. McCabe and Jeannette E. Laws McCabe Fund (M. Olson).

The costs of publication of this article were defrayed in part by the payment of page charges. This article must therefore be hereby marked *advertisement* in accordance with 18 U.S.C. Section 1734 solely to indicate this fact.

Note: D. Croft and M. Olson are currently at The Beatson Institute for Cancer Research, Glasgow, United Kingdom.

Requests for reprints: Michael F. Olson, The Beatson Institute for Cancer Research, Garscube Estate, Switchback Road, Glasgow G61 1BD, United Kingdom. E-mail: m.olson@beatson.gla.ac.uk.

established solid tumors and to model the increased ROCK signaling believed to occur at later stages of tumor progression, cells expressing ROCK:ER or KD:ER were grown as subcutaneous tumors to a significant diameter, and then mice were treated either with vehicle control or with tamoxifen to activate ROCK:ER within the tumor cells. When treated with vehicle, cells grew as tightly clustered well-defined nests around blood vessels. In contrast, tamoxifen treatment resulted in increased ROCK:ER kinase activity associated with dramatic tumor reorganization and aggressive spread of tumor cells into the surrounding stroma. Tumors with active ROCK:ER also had an increased number of CD31-positive endothelial cells and an increased density of functional blood vessels. *In vitro*, ROCK:ER activation resulted in cell contraction, disruption of adherens junctions, projection of actin-rich structures containing ezrin and CD44 from the apical surface, and dissociation of cell clusters leading to increased motility, events not observed in 4-HT–treated cells expressing KD:ER. The 4-HT–induced effects in ROCK:ER-expressing cells were blocked by the ROCK inhibitor Y-27632, indicating that ROCK activity was responsible for the effects on morphology and organization. These results reveal that ROCK activation is sufficient to affect epithelial cell characteristics resulting in tumor cell invasion and angiogenesis *in vivo*.

MATERIALS AND METHODS

Antibodies and Reagents. Antibody sources were as follows: phospho-MLC (Ser^{19}), phospho-MLC (Thr^{18}/Ser^{19}), phospho-ezrin (Thr^{567}), phospho-LIM kinase (LIMK) 1 (Thr^{508})/LIMK2 (Thr^{505}), and LIMK1 were from Cell Signaling Technologies (Beverley, MA); MLC (clone MY21), α-catenin, γ-catenin, and β-tubulin were from Sigma (St. Louis, MO); ezrin, MYPT1, and phospho-MYPT1 (Thr^{696}) were from Upstate Biotechnology (Lake Placid, NY); estrogen receptor α was from Santa Cruz Biotechnology (Santa Cruz, CA); paxillin was from BD Transduction Laboratories; CD44 was from Neomarkers; and pan-cadherin was from Zymed Laboratories (San Francisco, CA). Fluorescence-conjugated secondary antibodies were from Jackson Immunoresearch Laboratories, Inc. (West Grove, PA). Goat antimouse and goat antirabbit horseradish peroxidase antibodies were from Pierce (Rockford, IL). Texas Red-conjugated phalloidin was from Molecular Probes (Eugene, OR). 4-HT, tamoxifen, Polybrene, and puromycin were from Sigma. ROCK inhibitor Y-27632 was from Calbiochem (La Jolla, CA).

Cloning and Generation of Constructs. To construct conditionally regulated ROCKII (ROCK:ER), the catalytic domain of bovine ROCK (residues 5–553) was linked NH_2-terminally to enhanced green fluorescent protein (EGFP) and COOH-terminally to the hormone-binding domain of the murine estrogen receptor (hbER; a gift from Dr. M. McMahon, University of California San Francisco, San Francisco, CA). A kinase-dead version (KD:ER) was created by changing lysine 121 to glycine. Both ROCK constructs were subcloned into pBABEpuro.

Cell Transfection and Retroviral Infection. Retroviral constructs were transfected using LipofectAMINE (Life Technologies, Inc., Rockville, MD) into BOSC 293 packaging cells, and retrovirus was harvested after 40 hours. Ecotropic receptor-expressing HCT116 and LS174T colon carcinoma cells were infected with virus plus 4 μg/mL Polybrene and selected with 2.5 μg/mL puromycin.

Cell Culture and Western Blotting. HCT116 and LS174T cell lines expressing either KD:ER or ROCK:ER were grown in Dulbecco's modified Eagle's medium plus 10% fetal calf serum. Cells were placed in serum-free medium 24 hours before treatment with 4-HT (see the figure legends for concentrations) with or without 10 μmol/L Y-27632 for 16 hours. Cells were washed with PBS and then lysed in buffer containing 10 mmol/L Tris (pH 7.5), 5 mmol/L EDTA, 1% (v/v) Nonidet P-40, 0.5% (w/v) sodium deoxycholate, 40 mmol/L Na PP_i, 1 mmol/L Na_3VO_4, 50 mmol/L NaF, 1 mmol/L phenylmethylsulfonyl fluoride, 0.025% (w/v) SDS, and 150 mmol/L NaCl. Supernatants were clarified by centrifugation at 13,000 $\times$ *g* for 15 minutes. One hundred micrograms of each whole cell lysate were run on SDS-polyacrylamide gels, transferred to nitrocellulose membranes, and blocked in Tris-buffered saline containing 5% (w/v) dried milk before immunoblotting. Alternatively, to determine the levels of MLC, phospho-MLC, MYPT1, and phospho-MYPT1, cells were lysed directly in 1$\times$ Laemmli sample buffer. Samples were sonicated and boiled for 5 minutes, supernatant was clarified by centrifugation at 16,000 $\times$ *g* for 5 minutes, and an appropriate volume of the sample was electrophoresed and immunoblotted as described above.

Immunofluorescence. Cells were fixed for 15 minutes in 4% (w/v) *p*-formaldehyde (PFA) in PBS and then permeabilized for 15 minutes in 0.5% Triton X-100 in PBS. Primary antibodies as indicated were incubated for 60 minutes, followed by PBS washes and a 60-minute incubation with a corresponding fluorescence-labeled secondary antibody. Actin structures were visualized by staining with Texas Red-conjugated phalloidin (0.5 mg/mL). Confocal laser scanning microscopy was performed using a Bio-Rad MRC 1024 microscope and LaserSharp software (Bio-Rad, Hercules, CA). For ezrin staining, cells were washed with PBS (containing 0.9 mmol/L $CaCl_2$ and 0.5 mmol/L $MgCl_2$), incubated four times (30 seconds each) with 4-morpholineethanesulfonic acid extraction buffer [50 mmol/L 4-morpholineethanesulfonic acid, 3 mmol/L EGTA, 5 mmol/L $MgCl_2$, and 0.5% (w/v) Triton X-100 (pH 6.4)], and then fixed with 3% PFA. Immunofluorescence staining of tumor sections was carried out using rabbit polyclonal ezrin antibody, Texas Red-conjugated phalloidin, rat monoclonal CD31 antibody, and the appropriate fluorophore-conjugated secondary antibodies.

***In vitro* Kinase Assays.** KD:ER and ROCK:ER were immunoprecipitated from lysates using 3 μg of estrogen receptor α antibody per sample and protein G-Sepharose (Sigma) and assayed for histone H1 kinase activity as described previously (31). Reaction products were run on an 8% SDS-PAGE gel, transferred to nitrocellulose, and quantified using a Molecular Dynamics Storm PhosphorImager (Sunnyvale, CA). Estrogen receptor fusion protein levels were determined by Western blotting with estrogen receptor α antibody.

Subcutaneous Tumors. Tumor cells (10^6) were injected subcutaneously into 4- to 6-week–old male MF1 nude mice. Tumors were allowed to become established and grow to 0.7 cm in diameter (approximately 16 days), and then animals received daily intraperitoneal injections of either tamoxifen (1 mg per injection) or vehicle (corn oil) for 2, 6, or 14 days. Tumors were removed and processed for histochemical analysis, immunofluorescence, and *in vitro* kinase analysis. For histochemical analysis, excised tumors were fixed in 10% formol saline, and serial sections of paraffin-embedded tumors were stained with hematoxylin and eosin. Microscopy was carried out using a Zeiss Axioplan 2 microscope, and images were collected with a Photometrics Quantix camera and SmartCapture 2 software. For immunofluorescence, tumors were frozen in isopentane, and serial sections (8 μm) were cut. Sections were fixed in 4% PFA and permeabilized with 0.5% Triton X-100. After staining with primary antibody, the appropriate fluorescein isothiocyanate-conjugated secondary antibody and Texas Red-conjugated phalloidin were used. For *in vitro* analysis of kinase activity, tumors were snap frozen in liquid nitrogen. Using a mortar and pestle, tumor samples were crushed into a fine powder and lysed in buffer and assayed as described above.

Tumor Vascularization. Subcutaneous tumors of HCT116 cells were established and grown for 14 days as described above. Tumor-bearing mice received intravenous injection into the tail vein with 150 μL of 2 mg/mL Texas Red-conjugated tomato (*Lycopersicon esculentum*) lectin (Vector Laboratories, Burlingame, CA) in PBS. Ten minutes later, the mice were anesthetized and then perfused with 4% PFA in PBS (pH 7.4) intracardially. For confocal imaging of the vasculature, tumors were excised, embedded in OCT compound, frozen, cut with a cryostat into 60-μm sections, and mounted onto microscope slides. Mounted sections were fixed for 15 minutes in 4% PFA, permeabilized in 0.5% Triton X-100, costained with rat monoclonal CD31 antibody and fluorescein isothiocyanate-conjugated secondary antibody, and covered with a coverslip. Images of tumor vasculature were taken with Bio-Rad 1024 confocal microscope and LaserSharp software (Bio-Rad).

RESULTS

Conditional Activation of ROCK:ER by 4-Hydroxytamoxifen. To produce a conditionally regulated system to study the consequences of ROCK activation, we generated retroviral vectors encoding ROCK:ER and the kinase-dead version KD:ER by swapping the COOH-terminal negative regulatory portion of ROCK II with the

estrogen receptor hormone-binding domain (Fig. 1*A*, *hbER*). Specifically, we fused a constitutively active fragment (amino acids 5–553; data not shown) or a kinase-dead K121G mutant to EGFP and to the estrogen receptor hormone-binding domain, which can be stimulated with the estrogen analogs tamoxifen or 4-HT. The ROCK:ER and KD:ER retroviral vectors were each packaged as ecotropic virus and then stably introduced into ecotropic receptor (32) expressing HCT116 and LS174T colon carcinoma cells, which have a relatively low and intermediate level of active RhoA, respectively, relative to other nontransformed and tumor cell lines.[5] Intracellular localization of ROCK:ER, as determined by EGFP fluorescence, appeared to be diffuse throughout the cytoplasm, similar to the localization reported for endogenous ROCK II (33). To examine 4-HT regulation of ROCK kinase activity, serum-starved cells were treated with or without 1 μmol/L 4-HT for 16 hours, lysates from HCT116 and LS174T cells were prepared, and immunoprecipitated ROCK:ER or KD:ER was assayed for histone H1 phosphorylating activity (Fig. 1*B*, *top panel*). ROCK:ER immunoprecipitated from each cell line was responsive to 4-HT, with significant increases in kinase activity; in contrast, KD:ER showed no detectable induction of kinase activity. In the KD:ER- and ROCK:ER-expressing cell lines, the addition of 4-HT only modestly increased fusion protein expression (Fig. 1*B*, *middle panel*), indicating that the principal mechanism of ROCK:ER activation is increased specific activity with a lesser contribution by protein stabilization.

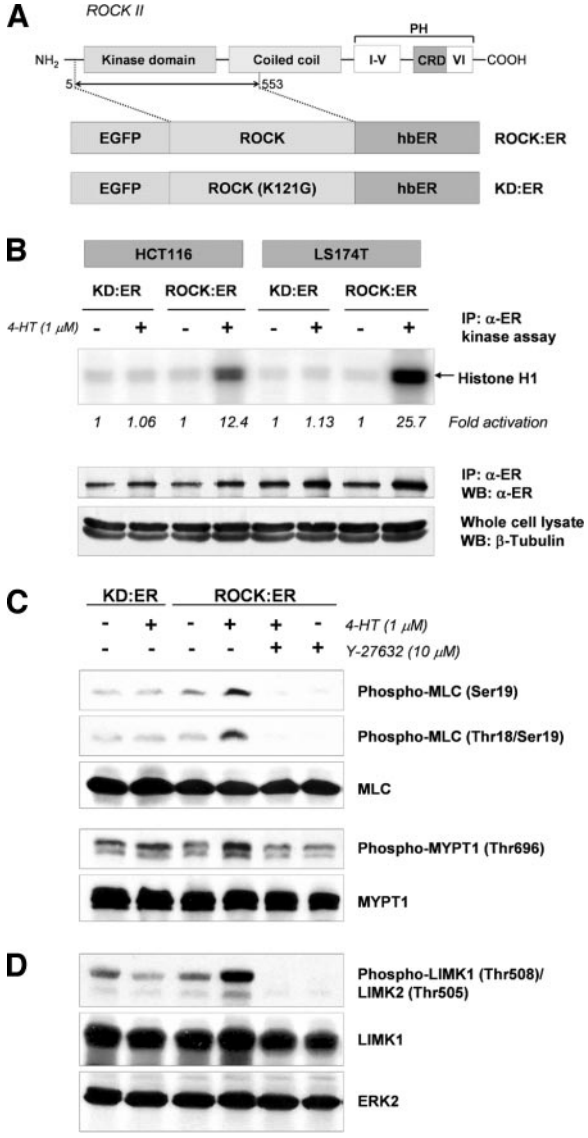

Fig. 1. 4-HT induces kinase activity in an estrogen receptor-regulated form of ROCK II. *A*. Conditionally regulated ROCK II (ROCK:ER) was generated by fusing residues 5 to 553, comprising the kinase domain, and a portion of the predicted coiled coil region, NH_2-terminally to EGFP and COOH-terminally to the estrogen receptor hormone-binding domain (*hbER*). A kinase-dead control version (KD:ER) was made by changing Lys^{121} to glycine (K121G). *PH*, pleckstrin homology domain; *CRD*, cysteine-rich domain. *B*. Stable HCT116 and LS174T cell lines expressing either kinase-dead KD:ER or ROCK:ER were left untreated or treated for 16 hours with 1 μmol/L 4-HT, after which cell lysates were prepared, and estrogen receptor fusion kinase activity was determined *in vitro*. KD:ER or ROCK:ER was immunoprecipitated with estrogen receptor α antibody from equal amounts of whole cell lysates, verified by Western blotting of lysates for β-tubulin (*bottom panel*), followed by a kinase assay with histone H1 as the substrate (*top panel*). Fold activation was calculated from the amount of histone H1 phosphorylation in the 4-HT–treated sample relative to the untreated sample. Western blot analysis with the estrogen receptor α antibody revealed similar amounts of estrogen receptor fusion protein were immunoprecipitated in each sample (*middle panel*). *C,* phospho-MLC (Ser^{19} and Thr^{18}/Ser^{19}), phospho-MYPT1 (Thr^{696}), or *D*, phospho-LIMK1 (Thr^{508})/LIMK2 (Thr^{505}) levels were determined by Western blotting lysates of serum-starved LS174T cells expressing KD:ER and ROCK:ER that were left untreated or treated with 4-HT, 4-HT + Y-27632, or Y-27632 alone as indicated for 16 hours.

Previous studies have shown that ROCK phosphorylates the regulatory MLC, the myosin-binding subunit (MYPT1) of MLC phosphatase, and LIMKs 1 and 2, thereby influencing the architecture of actin-myosin cytoskeletal structures. Serum-starved LS174T cells expressing KD:ER or ROCK:ER were treated with or without 1 μmol/L 4-HT in the presence or absence of 10 μmol/L Y-27632 for 16 hours, and then lysates were prepared by direct lysis. Immunoblot analysis with phospho-specific antibodies against MLC (Ser^{19} and Thr^{18}/Ser^{19}), MYPT1 (Thr^{696}), and LIMK1/LIMK2 (Thr^{508}/Thr^{505}) revealed that ROCK:ER activation led to increased phosphorylation of each protein (Fig. 1*C* and *D*). In contrast, 4-HT treatment of KD:ER-expressing cells did not alter the phosphorylation of these proteins. Coadministration of 10 μmol/L Y-27632 with 1 μmol/L 4-HT prevented the MLC, MYPT1, and LIMK1/2 phosphorylation induced by ROCK:ER activation. Moreover, Y-27632 treatment abolished basal phosphorylation of MLC and LIMK. Similar results were obtained with HCT116 cells expressing ROCK:ER and KD:ER (data not shown). Together, these results indicate that conditionally active ROCK can be activated by 4-HT, leading to the phosphorylation of substrates, previously shown to be substrates of endogenous ROCK, that are responsible for alterations to the actin-myosin cytoskeleton and the regulation of cell morphology.

KD:ER-expressing HCT116 or LS174T Cells Promote Tumor Cell Invasion *In vivo*. We next investigated the effects of ROCK:ER activation on cells grown as subcutaneous tumors. Nude mice were injected with ROCK:ER- or KD:ER-expressing HCT116 or LS174T cells into the left hind leg; tumors were allowed to establish (~0.7 cm in diameter), and then mice were treated daily by intraperitoneal injection with either 1 mg of tamoxifen or with vehicle control (corn oil) until the tumors reached 1.5 cm in diameter. Tumor size did not differ between tamoxifen- and vehicle-treated mice throughout the course of the experiment (data not shown). Analysis of ROCK:ER kinase activity revealed that tamoxifen treatment induced activity only slightly (1.5-fold) after 2 days (Fig. 2*A*). However, after 6 and 14 days of tamoxifen treatment, kinase activity had increased 2.7-fold and 4.5-fold, respectively, above vehicle-treated tumors. The 14 day time point was chosen for subsequent tumor experiments. Western blot analysis showed that ROCK:ER was present in each tumor lysate and immunoprecipitate (Fig. 2*A*, *bottom two panels*).

Histologic analysis of subcutaneous tumors from vehicle-treated mice revealed that HCT116 cells grew as defined tightly organized clusters around blood vessels, often surrounded by areas of necrosis (Fig. 2*B*, *top left panel*). Gross morphologic analysis showed that the

[5] E. Sahai, unpublished observations.

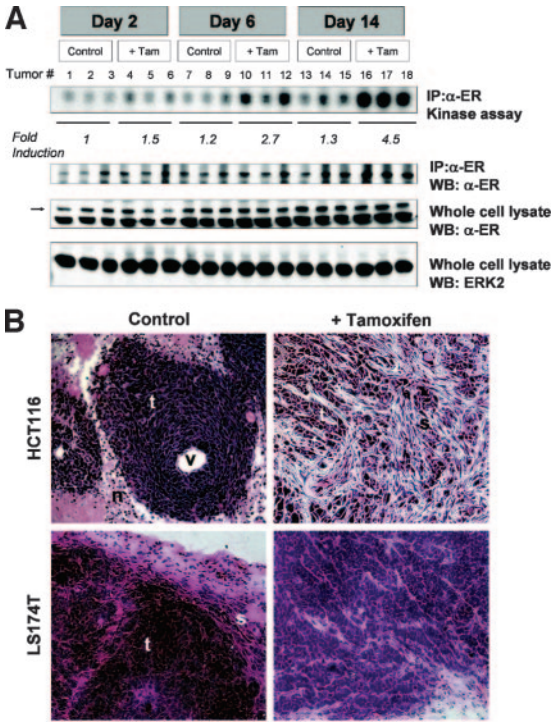

Fig. 2. ROCK:ER kinase activation and cell dissemination induced by tamoxifen treatment in subcutaneous ROCK:ER tumors. *A*. HCT116 ROCK:ER (10^6) cells were injected subcutaneously into male nude mice. Tumors were allowed to become established (diameter, 0.7 cm), and then the animals received daily injection with tamoxifen (1 mg per injection) or corn oil vehicle (*Control*) for either 2, 6, or 14 days. Subcutaneous tumors were removed and snap frozen in liquid nitrogen. Tumor lysates were prepared, and ROCK:ER was immunoprecipitated with anti-estrogen receptor α antibody; then *in vitro* kinase assays were performed using histone H1 as the substrate (*top panel*). Fold induction was calculated from histone H1 phosphorylation in the tamoxifen-treated samples relative to control at day 2. Western blotting with estrogen receptor α antibody indicates the amount of immunoprecipitated ROCK:ER protein in each sample, whereas Western blotting of whole cell lysate with estrogen receptor α indicates the ROCK:ER expression levels (indicated by the *arrow*). Blotting for ERK2 was used as loading control in whole cell lysate. *B*. HCT116 or LS174T cells expressing ROCK:ER were injected subcutaneously and treated as described above. Tumors were collected on reaching 1.5 cm in diameter and fixed in 10% formol saline, and then serial sections of paraffin-embedded tumors were stained with hematoxylin and eosin. Microscopy was carried out using a Zeiss Axioplan 2 microscope, and images were collected with a Photometrics Quantix camera and SmartCapture 2 software. *n*, areas of necrosis; *s*, stroma; *t*, epithelial cells in the tumor mass; *v*, blood vessels.

central tumor core contained necrotic regions, with tumor cell clusters being found mainly in a surrounding viable rim (data not shown). In contrast, ROCK:ER-expressing HCT116 tumors treated with tamoxifen resulted in a loss of ordered cell clusters with dissemination of tumor cells and mixing with the surrounding stroma (Fig. 2*B*, *top right panel*). In addition, central necrosis observed in untreated tumors was markedly reduced in tamoxifen-treated tumors. Similar results were obtained in tumors of LS174T ROCK:ER-expressing cells (Fig. 2*B*, *bottom panels*), although untreated tumors were somewhat more loosely organized, and reorganization induced by tamoxifen was less dramatic. Tumors derived from KD:ER-expressing HCT116 or LS174T cells showed no obvious morphologic changes after tamoxifen treatment (data not shown).

Given that ROCK is a critical regulator of actin-myosin structures, we examined how ROCK:ER affected the organization of F-actin in HCT116 tumors. F-actin was found throughout the tumor, with increased intensity at the edges (Fig. 3*A*, *top left panel*). However, in tumors from tamoxifen-treated mice, F-actin staining was intense throughout the tumor (Fig. 3*A*, *bottom left panel*). We next examined how ROCK:ER activation influenced the distribution and localization of the actin-binding protein ezrin, which binds to membrane proteins, such as CD44, thereby enabling it to organize specialized membrane domains. Ezrin has been shown to be significantly up-regulated in metastatic tumors and to contribute significantly to metastasis (34, 35). In addition, the rounded mode of tumor cell motility through three-dimensional matrices that is blocked by ROCK inhibitor is also dependent on ezrin function (22). Ezrin was diffusely distributed within cells and can be seen most intensely at the tumor periphery in control tumors, with a decreasing expression gradient until the areas around central blood vessels displayed minimal immunoreactivity (Fig. 3*A*, *top middle panel*). After ROCK activation, ezrin staining was more evenly dispersed throughout the section, with a more punctate cellular distribution (Fig. 3*A*, *bottom middle panel*). The merged images (Fig. 3*A*, *right panels*) revealed that CD31-positive endothelial cells (colored *blue*, indicated by *white arrows*) were found at the center of tumor nests in control tumors but were more densely distributed after tamoxifen treatment. Together, these data indicate that activation of ROCK signaling *in vivo* is sufficient to promote the dissemination of cells from solid tumors.

Given the increased density of CD31-positive endothelial cells and the decrease in central necrosis in tumors after ROCK:ER activation,

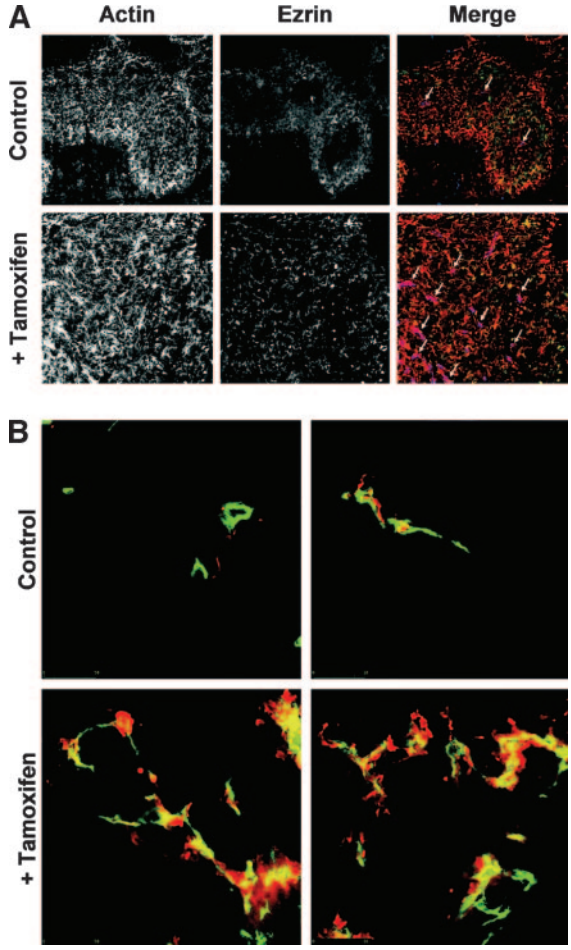

Fig. 3. ROCK:ER activation promotes increased F-actin structures, ezrin redistribution, and increased vascularization in HCT116-derived subcutaneous tumors. *A*. Serial sections of tumors snap frozen in isopentane were fixed and stained for F-actin and ezrin. A merged image of ezrin (*green*) and F-actin (*red*) is shown in the *right panels* with CD31-positive blood vessels (*blue*) indicated by *arrows*. *B*. Mice received injection of Texas Red-conjugated tomato (*L. esculentum*) lectin into the tail vein 10 minutes before sacrifice. Mice were anesthetized and perfused with 4% PFA intracardially, and then tumors were excised, embedded in OCT compound, frozen, cut with a cryostat into 60-μm sections, and mounted onto microscope slides. Mounted sections were fixed for 15 minutes in 4% PFA, permeabilized in 0.5% Triton X-100, and costained with rat monoclonal CD31 antibody and fluorescein isothiocyanate-conjugated secondary antibody.

we examined whether there were greater densities of functional blood vessels. ROCK:ER-expressing HCT116 cells were grown as described in Figs. 2*B* and 3*A*, and then on the final day, Texas Red-conjugated lectin was injected into the tail vein. After 10 minutes to allow for tracer circulation, mice were anesthetized and perfused with 4% PFA, and tumor samples were processed. As a positive control, liver blood vessel labeling was examined in all animals (data not shown). Consistent with Figs. 2*B* and 3*A*, the *top panels* in Fig. 3*B* show confocal microscopic images of two independent tumor sections from control-treated mice that neither have extensive CD31-positive endothelial cell staining nor show extensive penetration by the fluorescence-labeled lectin. In contrast, tumors with active ROCK:ER have a higher density of CD31-positive endothelial cells and significantly higher fluorescent lectin infiltration. Notably, lectin penetration traveled beyond blood vessel boundaries as demarcated by CD31 staining, indicating that these vessels were not fully functional barriers against extravasation. These data reveal that in addition to promoting cell dissemination from solid tumors, ROCK signaling contributes positively to tumor angiogenesis.

ROCK:ER Activation Promotes Morphologic and Cytoskeletal Responses. To ascertain how ROCK:ER induced the striking effects on tumor organization and vascularization *in vivo*, we examined the consequences of ROCK:ER activation on cell morphology, motility, cytoskeletal structures, and the distribution of adherens junction and focal adhesion proteins. To examine morphology and motility, LS174T cells expressing ROCK:ER were placed in serum-free medium (Fig. 4*A*, *top panels*) or in serum-free medium containing 1 μmol/L 4-HT for 16 hours (Fig. 4*A*, *bottom panels*), and a phase-contrast microscopic time series was acquired at 1-minute intervals for 12 hours. The untreated ROCK:ER-expressing cells grew as "cobblestone" colonies, with little lateral movement and no evidence of cells breaking free from the colony. In contrast, 4-HT–treated cells had significantly altered morphology; some cells flattened, whereas others rounded. The bonds between cells were reduced, and cells dynamically disassociated and reassociated with neighbors. As a result, some cells moved randomly, either singly or in partnership. These results indicate that ROCK:ER activation facilitates motility by freeing epithelial cells from constraints imposed by adjacent cells.

To determine how ROCK activation affects actin cytoskeletal structures and the distribution of adherens junction and focal adhesion proteins, LS174T cells expressing ROCK:ER (Fig. 4*B*) or KD:ER (data not shown) were serum starved and then left untreated or treated with 1 μmol/L 4-HT, either with or without 10 μmol/L Y-27632, for 16 hours and then fixed and stained. Experiments with HCT116 cells were done in parallel, and similar results were obtained (data not shown). In the absence of 4-HT, LS174T ROCK:ER cells grew as epithelial colonies with F-actin structures confined to cortical regions. However, 4-HT altered cell morphology, with significant numbers of cells flattening out and containing thick bundles of actin stress fibers (Fig. 4*B*, *top panels*). In addition, some cells rounded up with actin-rich membrane blebs; these blebbing cells had a thick central hub of actin from which stress fibers emanated (data not shown). The induction of actin structures by 4-HT was dependent on ROCK because it could be inhibited by coadministration with Y-27632 and did not occur in KD:ER-expressing cells.

Rho signaling is responsible for regulating adherens junctions between epithelial cells; the Rho effector mDia1 acts to ensure a dynamically stable interface between cells and the maintenance of adherens junction complexes, whereas ROCK activation leads to adherens junction disruption (36). Adherens junctions are composed of cadherins, transmembrane proteins that physically link together cells, and catenins, which form complexes that tether cadherins to the actin cytoskeleton (37). Fig. 4*B* shows that the actin binding α-catenin

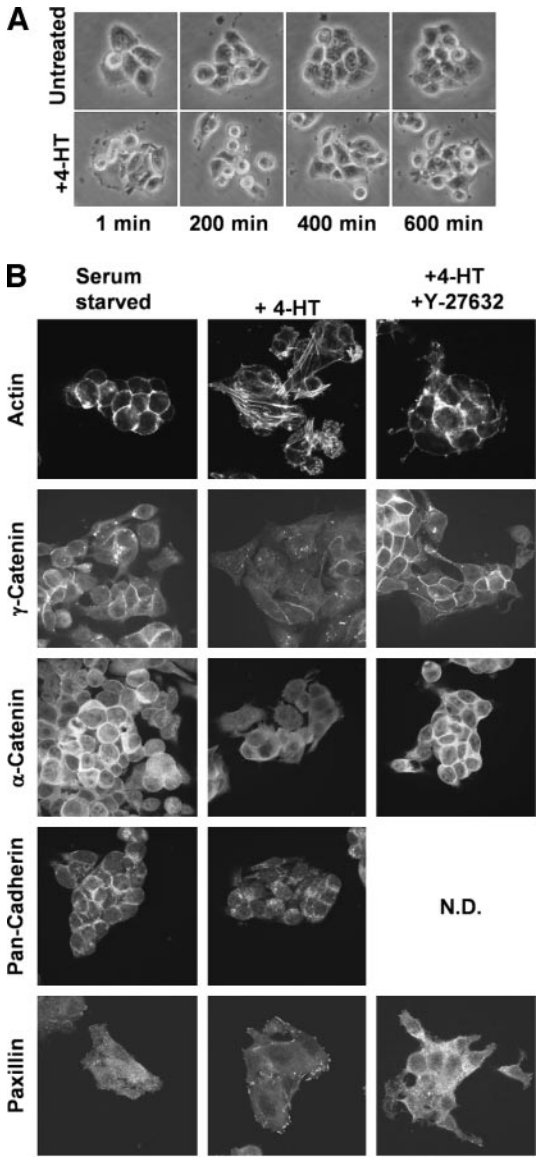

Fig. 4. ROCK:ER activation promotes motility *in vitro* and induces actin stress fiber formation, disruption of adherens junctions, and focal adhesion formation. *A*. LS174T cells expressing ROCK:ER were placed in serum-free medium (*top panels*) or in serum-free medium containing 1 μmol/L 4-HT (*bottom panels*) for 16 hours. Time series of phase-contrast microscopic images were acquired at 1-minute intervals for 12 hours, and images gathered at 200-minute intervals are shown. *B*. Serum-starved ROCK:ER LS174T cells were either left untreated (*Serum starved*) or treated with 1 μmol/L 4-HT or 1 μmol/L 4-HT + 10 μmol/L Y-27632 for 16 hours. Cells were then fixed and stained with phalloidin for F-actin or with antibodies against γ-catenin, α-catenin, pan-cadherin, or paxillin as indicated. *N.D.*, not determined.

and the cadherin binding γ-catenin localized to the cell junctions in LS174T cells. The activation of ROCK:ER with 4-HT removed α-catenin and γ-catenin from cell–cell junctions. Y-27632 prevented the 4-HT–induced redistribution, whereas 4-HT was without effect in KD:ER-expressing cells. Consistent with these findings, staining with pan-cadherin antibody revealed that cadherins were similarly removed from cell–cell borders. We were unable to identify which cadherin proteins were redistributed, although LS174T cells do express the archetypal epithelial E-cadherin (38). The loss of adherens junction proteins from cell–cell junctions likely results from ROCK:ER promoting actin-myosin contractility (36). Microarray analysis did not reveal changes of gene expression induced by ROCK:ER activation for any of the adherens junction proteins (data not shown).

We also examined focal adhesions in 4-HT–treated ROCK:ER- or

KD:ER-expressing cells by immunolabeling paxillin (Fig. 4*B*). ROCK activation resulted in increased paxillin clustering in focal adhesions, which could be blocked with Y-27632 in ROCK:ER-expressing cells and was not affected by 4-HT in KD:ER-expressing cells.

ROCK Activation Relocalizes Ezrin and CD44. As shown in Fig. 3*A*, we found that ROCK:ER activation affected localization of ezrin in tumors, a protein that contributes to metastasis (34, 35). Rho has been reported to regulate the intracellular distribution of ezrin; however, there is disagreement regarding whether it is mediated by ROCK (39, 40). Using ROCK:ER and Y-27632, we examined whether ROCK regulated ezrin localization. In LS174T cells, narrow optical sections obtained by confocal microscopy revealed that ezrin is localized mainly to small membrane projections that emanate from the basal surface and, to a lesser extent, the apical surface (Fig. 5*A*). The addition of 4-HT to ROCK:ER-expressing cells resulted in ezrin redistribution to apical and basolateral surfaces, which was blocked by Y-27632 (data not shown). Ezrin colocalized with F-actin at these membrane projections (data not shown). ROCK:ER activation also promoted the movement of CD44 to the apical surface, where it colocalized with ezrin in membrane projections (Fig. 5*B*, merged images show CD44 in *red* and ezrin in *green*). No changes in ezrin or CD44 expression were detected by microarray analysis after ROCK:ER activation (data not shown).

Ezrin exists in a closed conformation due to inhibitory "head to tail" associations; phosphorylation on Thr^{567} and binding of phosphatidylinositol 4,5-bisphosphate to an NH_2-terminal domain opens and unmasks actin and membrane binding sites (41). ROCK has been reported to directly phosphorylate ezrin at Thr^{567} (40, 42); however, we found that 4-HT treatment of ROCK:ER-expressing cells, either alone or in combination with Y-27632, had no effect on Thr^{567} phosphorylation (Fig. 6*A*). To determine whether alternative Rho signaling pathway(s) regulated Thr^{567} phosphorylation, we used a cell-permeable *Clostridium botulinum* C3 toxin (Tat-C3) to inactivate Rho (31). Tat-C3 modified all detectable RhoA protein, as seen by the mobility shift (Fig. 6*A*), but it did not affect Thr^{567} phosphorylation. Treatment with 4-HT, with or without Y-27632, did not affect Thr^{567} phosphorylation in the context of Rho inhibition. Treatment with staurosporine, a potent and broad specificity serine/threonine kinase inhibitor, reduced Thr^{567} phosphorylation, indicating that it was likely phosphorylated by a distinct kinase (Fig. 6*B*, *left panel*). We validated the phosphorylation dependence of the antibody by treating immunoprecipitated ezrin with phosphatase (Fig. 6*B*, *right panel*). These results indicated that ezrin Thr^{567} phosphorylation is not mediated by ROCK and that ROCK:ER-induced relocalization is mediated by alternative mechanisms.

Given that ROCK did not regulate ezrin Thr^{567} phosphorylation, we

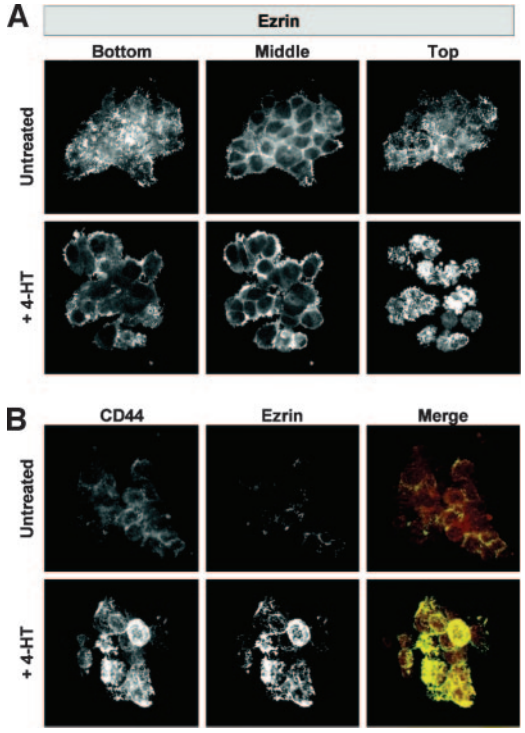

Fig. 5. ROCK:ER activation induces the redistribution of ezrin and CD44. *A*. Serum-starved LS174T ROCK:ER cells were either left untreated or treated with 1 μmol/L 4-HT as indicated for 16 hours. Cells were washed with PBS (containing 0.9 mmol/L $CaCl_2$ and 0.5 mmol/L $MgCl_2$), rinsed four times for 30 seconds with 4-morpholineethanesulfonic acid extraction buffer, fixed immediately with 4% PFA, and then stained for ezrin. Confocal laser scanning microscopy was used to obtain optical slices of the bottom, middle, and top of cells. *B*. Serum-starved LS174T ROCK:ER cells were either left untreated or treated with 1 μmol/L 4-HT as indicated for 16 hours. Cells were processed as described above and then costained for CD44 and ezrin. Confocal microscopy was used to obtain a series of optical slices; only the top (apical surface) image is shown. Merged images of CD44 (*red*) and ezrin (*green*) are shown in the *right panels*; colocalized proteins appear *yellow*.

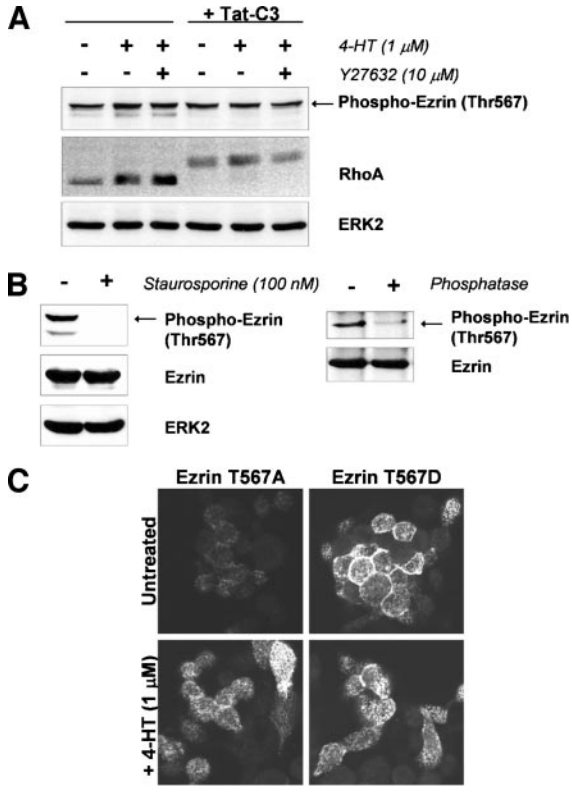

Fig. 6. Ezrin phosphorylation at Thr^{567} is not regulated by Rho/ROCK signaling and is not required for ROCK induced redistribution. *A*. To determine whether ROCK or Rho contributed to the regulation of ezrin phosphorylation on Thr^{567}, serum-starved LS174T ROCK:ER cells were either left untreated or treated with 1 μmol/L 4-HT, with or without 10 μmol/L Y-27632, after 24 hours in the absence or presence of the cell-permeable Tat-C3, as indicated for 16 hours. Lysates were Western blotted for phospho-ezrin (Thr^{567}), RhoA, and ERK2. *B*. Serum-starved LS174T ROCK:ER cells were either untreated or treated with 100 nmol/L staurosporine for 20 minutes, and then lysates were Western blotted for phospho-ezrin (Thr^{567}), total ezrin, and ERK2. Lysates were prepared from serum-starved LS174T ROCK:ER cells, and then ezrin protein was immunoprecipitated with a polyclonal antibody. The immunoprecipitated material was divided in half; one portion was left untreated, and the other was treated for 30 minutes with calf intestine phosphatase. The two samples were Western blotted for phospho-ezrin (Thr^{567}) and total ezrin. *C*. ROCK:ER-expressing LS174T cells were transduced with retrovirus encoding vesicular stomatitis virus glycoprotein epitope–tagged wild-type, nonphosphorylatable T567A or phospho-mimetic T567D ezrin. Stable pools of transduced cells were serum starved and then either left untreated or treated with 1 μmol/L 4-HT for 16 hours. After fixation and permeabilization, cells were stained with anti–vesicular stomatitis virus glycoprotein epitope epitope antibody. Confocal microscopic images were gathered as a series of optical slices, and only the apical surfaces of the T567A and T567D mutants are shown, from untreated or 4-HT–treated cells.

examined whether Thr[567] phosphorylation was required for ROCK:ER-induced ezrin redistribution. Vesicular stomatitis virus glycoprotein epitope–tagged wild-type ezrin, as well as nonphosphorylatable T567A and phospho-mimetic T567D mutants, was introduced by retroviral transduction into LS174T ROCK:ER cells. Transduced clones were stained for ezrin localization at the apical surface with anti–vesicular stomatitis virus glycoprotein epitope antibody either with or without 4-HT treatment. In unstimulated cells, wild-type (data not shown) and T567A ezrin (Fig. 6*C*, *top left panel*) were diffusely localized with little at the apical surface, consistent with previous reports (43) the phospho-mimetic T567D mutant was constitutively on the apical surface (Fig. 6*C*, *top right panel*). Surprisingly, ROCK:ER activation resulted in the relocalization of wild-type (data not shown) as well as nonphosphorylatable T567A ezrin (Fig. 6*C*, *bottom left panel*) to apical projections. 4-HT did not alter T567D ezrin distribution. These results indicate that ROCK does not contribute significantly to ezrin Thr[567] phosphorylation and that ROCK-induced ezrin redistribution does not require phosphorylation of this site.

DISCUSSION

Accumulating clinical and experimental data suggest that RhoA and RhoC, working through the ROCK protein kinases, contribute to the invasive and metastatic abilities of some tumor cells. ROCK inhibitors, such as Y-27632 or WF-536, have been used in some studies; although these inhibitors are potent and selective, it remains a possibility that additional kinases targeted by these compounds, such as PRK/PKN (44), also contribute to metastasis. In addition, administration of ROCK inhibitors to whole animals may block tumor cell invasion by enhancing the barrier function of host cell layers (29, 30). Rather than use an inhibitor-based approach, in which one moves away from a positive biological end point, we wished to specifically activate ROCK signaling to determine whether it was possible to move toward a given positive outcome, in this case, increased tumor cell dissemination. In addition, we wished to replicate the increased Rho and ROCK signaling that occurs as a late event during tumor progression. For these reasons, we created the conditionally activated ROCK:ER system, which permitted us to allow tumors to become established and grow before switching on this signaling pathway. In this manner, we were able to determine that activating ROCK in established tumors was sufficient to promote increased filamentous actin structures, redistribution of the actin-binding protein ezrin, and the dissemination of cells from solid tumors into the surrounding stroma. We also found that ROCK activation increased the number of CD31-positive endothelial cells within the tumor, resulting in an increased density of functional, albeit leaky, blood vessels.

We attempted to determine whether ROCK activation induced expression of angiogenic factors. We compared gene expression profiles by microarray analysis of HCT116 and LS174T cells expressing either ROCK:ER or KD:ER, in the absence or presence of 4-HT, to identify ROCK-regulated transcriptional targets. However, no genes common between the two cell lines were specifically induced by 4-HT in ROCK:ER-expressing cells and not in KD:ER-expressing cells (data not shown). We also found no significant effect of ROCK:ER activation on VEGF expression in HCT116 cells grown in tissue culture by enzyme-linked immunosorbent assay or in tumor sections by immunohistochemistry (data not shown). Despite these negative data, we cannot rule out the possibility that Rho and ROCK regulate the expression of angiogenic factors as suggested previously (45). Alternatively, ROCK activation may passively facilitate angiogenesis by increasing the plasticity of the tumor. By reducing the strength of cell–cell interactions and aiding the movement of tumor cells, ROCK may enable endothelial cells to more easily penetrate the tumor mass once they have been recruited by factors produced in response to hypoxic conditions.

We examined whether ROCK:ER activation influenced ezrin distribution because of discrepancies between previous studies (39, 40, 42) and the significant contribution made by ezrin to promoting metastasis (34, 35). ROCK:ER activation was sufficient to induce the redistribution of ezrin to projections at the apical surface of cells, where it colocalized with the transmembrane protein CD44. We also found that ROCK:ER activation resulted in ezrin redistribution in subcutaneous tumors. Surprisingly, we observed that neither ROCK nor Rho affected phosphorylation of ezrin on Thr[567], a site in the COOH terminus believed to be critical for converting ezrin from an inactive closed conformation to an active open conformation. Instead, we found that this site was constitutively phosphorylated by a staurosporine-sensitive kinase and that ROCK:ER-induced redistribution of ezrin was not dependent on phosphorylation of Thr[567]. There are a number of possibilities that may account for these results. ROCK may regulate ezrin localization through direct phosphorylation of alternative sites, such as the presumptive PKA site Ser[66] (46) or the CDK5 site Thr[235] (47). Our attempts to determine whether ROCK influenced Thr[235] phosphorylation were unsuccessful (data not shown). ROCK might also influence ezrin distribution by influencing phosphorylation at alternative sites, such as Tyr[145], by affecting the activity of other kinases and/or phosphatases (48, 49). Alternatively, the ROCK:ER-induced ezrin relocalization might be phosphorylation independent (50); instead, it might result from the ROCK-induced redistribution of ezrin-associated proteins such as CD44 or because of changes to actin cytoskeletal structures.

In summary, we have used a conditionally active form of ROCK to examine the consequences of activating this signaling pathway in established subcutaneous tumors. We found that activating ROCK:ER affected the organization of the tumors, with cells dissociated from the tumor mass and significant dissemination into surrounding stroma. We also observed increased filamentous actin, redistribution of ezrin, and greater densities of CD31-positive functional blood vessels. The absence of significant changes in gene expression induced by activation of ROCK:ER suggests that the positive effects on tumor invasion and angiogenesis are due to direct changes in cytoskeletal regulation, and not to the activation of a transcriptional program These results suggest that the increased levels of RhoA, RhoC, ROCK I, and ROCK II observed during tumor progression are likely selected for in order to enhance certain tumor properties that allow continued tumor growth, namely, reduced associations between tumor cells that permit movement and the penetration of the tumor mass by endothelial cells and consequent neovascularization. These results indicate that inhibiting ROCK function would be an efficacious chemotherapeutic strategy that would target both tumor metastasis and angiogenesis.

ACKNOWLEDGMENTS

We thank Dr. Mathew Coleman for Tat-C3 protein, Dr. Martin McMahon for the EGFP:Raf:ER construct, Dr. Richard Lamb (Institute of Cancer Research, London, United Kingdom) for polyclonal ezrin antibody, and Dr. Monique Arpin (Institut Curie, Paris, France) for ezrin constructs. We also thank Sue Clinton for preparing tumor sections.

REFERENCES

1. Etienne-Manneville S, Hall A. Rho GTPases in cell biology. Nature (Lond) 2002; 420:629–35.
2. Sahai E, Marshall CJ. RHO-GTPases and cancer. Nat Rev Cancer 2002;2:133–42.
3. Kamai T, Arai K, Sumi S, et al. The rho/rho-kinase pathway is involved in the progression of testicular germ cell tumour. BJU Int 2002;89:449–53.

4. Adnane J, Muro-Cacho C, Mathews L, Sebti SM, Munoz-Antonia T. Suppression of rho B expression in invasive carcinoma from head and neck cancer patients. Clin Cancer Res 2002;8:2225–32.
5. Kleer CG, van Golen KL, Zhang Y, et al. Characterization of RhoC expression in benign and malignant breast disease: a potential new marker for small breast carcinomas with metastatic ability. Am J Pathol 2002;160:579–84.
6. Kamai T, Tsujii T, Arai K, et al. Significant association of Rho/ROCK pathway with invasion and metastasis of bladder cancer. Clin Cancer Res 2003;9:2632–41.
7. Horiuchi A, Imai T, Wang C, et al. Up-regulation of small GTPases, RhoA and RhoC, is associated with tumor progression in ovarian carcinoma. Lab Investig 2003;83: 861–70.
8. Marionnet C, Lalou C, Mollier K, et al. Differential molecular profiling between skin carcinomas reveals four newly reported genes potentially implicated in squamous cell carcinoma development. Oncogene 2003;22:3500–5.
9. Wang W, Yang LY, Yang ZL, Huang GW, Lu WQ. Expression and significance of RhoC gene in hepatocellular carcinoma. World J Gastroenterol 2003;9:1950–3.
10. Shikada Y, Yoshino I, Okamoto T, et al. Higher expression of RhoC is related to invasiveness in non-small cell lung carcinoma. Clin Cancer Res 2003;9:5282–6.
11. Kondo T, Sentani K, Oue N, et al. Expression of RHOC is associated with metastasis of gastric carcinomas. Pathobiology 2004;71:19–25.
12. Pan Y, Bi F, Liu N, et al. Expression of seven main Rho family members in gastric carcinoma. Biochem Biophys Res Commun 2004;315:686–91.
13. Clark EA, Golub TR, Lander ES, Hynes RO. Genomic analysis of metastasis reveals an essential role for RhoC. Nature (Lond) 2000;406:532–5.
14. Zhou J, Zhao LQ, Xiong MM, et al. Gene expression profiles at different stages of human esophageal squamous cell carcinoma. World J Gastroenterol 2003;9:9–15.
15. Kaneko K, Satoh K, Masamune A, Satoh A, Shimosegawa T. Expression of ROCK-1 in human pancreatic cancer: its down-regulation by morpholino oligo antisense can reduce the migration of pancreatic cancer cells in vitro. Pancreas 2002;24:251–7.
16. Wang W, Wyckoff JB, Frohlich VC, et al. Single cell behavior in metastatic primary mammary tumors correlated with gene expression patterns revealed by molecular profiling. Cancer Res 2002;62:6278–88.
17. Coleman ML, Marshall CJ, Olson MF. RAS and RHO GTPases in G1-phase cell-cycle regulation. Nat Rev Mol Cell Biol 2004;5:355–66.
18. Riento K, Ridley AJ. Rocks: multifunctional kinases in cell behaviour. Nat Rev Mol Cell Biol 2003;4:446–56.
19. Leung T, Chen XQ, Manser E, Lim L. The p160 RhoA-binding kinase ROK alpha is a member of a kinase family and is involved in the reorganization of the cytoskeleton. Mol Cell Biol 1996;16:5313–27.
20. Uehata M, Ishizaki T, Satoh H, et al. Calcium sensitization of smooth muscle mediated by a Rho-associated protein kinase in hypertension. Nature (Lond) 1997; 389:990–4.
21. Speck O, Hughes SC, Noren NK, Kulikauskas RM, Fehon RG. Moesin functions antagonistically to the Rho pathway to maintain epithelial integrity. Nature (Lond) 2003;421:83–7.
22. Sahai E, Marshall CJ. Differing modes of tumour cell invasion have distinct requirements for Rho/ROCK signalling and extracellular proteolysis. Nat Cell Biol 2003;5: 711–9.
23. Itoh K, Yoshioka K, Akedo H, et al. An essential part for Rho-associated kinase in the transcellular invasion of tumor cells. Nat Med 1999;5:221–5.
24. Genda T, Sakamoto M, Ichida T, et al. Cell motility mediated by rho and Rho-associated protein kinase plays a critical role in intrahepatic metastasis of human hepatocellular carcinoma. Hepatology 1999;30:1027–36.
25. Takamura M, Sakamoto M, Genda T, et al. Inhibition of intrahepatic metastasis of human hepatocellular carcinoma by Rho-associated protein kinase inhibitor Y-27632. Hepatology 2001;33:577–81.
26. Somlyo AV, Bradshaw D, Ramos S, et al. Rho-kinase inhibitor retards migration and in vivo dissemination of human prostate cancer cells. Biochem Biophys Res Commun 2000;269:652–9.
27. Nakajima M, Hayashi K, Egi Y, et al. Effect of Wf-536, a novel ROCK inhibitor, against metastasis of B16 melanoma. Cancer Chemother Pharmacol 2003;52:319–24.
28. Nakajima M, Hayashi K, Katayama K, et al. Wf-536 prevents tumor metastasis by inhibiting both tumor motility and angiogenic actions. Eur Pharmacol 2003;459: 113–20.
29. Wojciak-Stothard B, Potempa S, Eichholtz T, Ridley AJ. Rho and Rac but not Cdc42 regulate endothelial cell permeability. J Cell Sci 2001;114:1343–55.
30. Nakajima M, Katayama K, Tamechika I, et al. WF-536 inhibits metastatic invasion by enhancing the host cell barrier and inhibiting tumour cell motility. Clin Exp Pharmacol Physiol 2003;30:457–63.
31. Coleman ML, Sahai EA, Yeo M, et al. Membrane blebbing during apoptosis results from caspase-mediated activation of ROCK I. Nat Cell Biol 2001;3:339–45.
32. Albritton LM, Tseng L, Scadden D, Cunningham JM. A putative murine ecotropic retrovirus receptor gene encodes a multiple membrane-spanning protein and confers susceptibility to virus infection. Cell 1989;57:659–66.
33. Leung T, Manser E, Tan L, Lim L. A novel serine/threonine kinase binding the Ras-related RhoA GTPase which translocates the kinase to peripheral membranes. J Biol Chem 1995;270:29051–4.
34. Khanna C, Wan X, Bose S, et al. The membrane-cytoskeleton linker ezrin is necessary for osteosarcoma metastasis. Nat Med 2004;10:182–6.
35. Yu Y, Khan J, Khanna C, et al. Expression profiling identifies the cytoskeletal organizer ezrin and the developmental homeoprotein Six-1 as key metastatic regulators. Nat Med 2004;10:175–81.
36. Sahai E, Marshall CJ. ROCK and Dia have opposing effects on adherens junctions downstream of Rho. Nat Cell Biol 2002;4:408–15.
37. Perez-Moreno M, Jamora C, Fuchs E. Sticky business: orchestrating cellular signals at adherens junctions. Cell 2003;112:535–48.
38. Barshishat M, Polak-Charcon S, Schwartz B. Butyrate regulates E-cadherin transcription, isoform expression and intracellular position in colon cancer cells. Br J Cancer 2000;82:195–203.
39. Matsui T, Yonemura S, Tsukita S. Activation of ERM proteins in vivo by Rho involves phosphatidyl-inositol 4-phosphate 5-kinase and not ROCK kinases. Curr Biol 1999;9:1259–62.
40. Tran Quang C, Gautreau A, Arpin M, Treisman R. Ezrin function is required for ROCK-mediated fibroblast transformation by the Net and Dbl oncogenes. EMBO J 2000;19:4565–76.
41. Fievet BT, Gautreau A, Roy C, et al. Phosphoinositide binding and phosphorylation act sequentially in the activation mechanism of ezrin. J Cell Biol 2004;164:653–9.
42. Matsui T, Maeda M, Doi Y, et al. Rho-kinase phosphorylates COOH-terminal threonines of ezrin/radixin/moesin (ERM) proteins and regulates their head-to-tail association. J Cell Biol 1998;140:647–57.
43. Gautreau A, Louvard D, Arpin M. Morphogenic effects of ezrin require a phosphorylation-induced transition from oligomers to monomers at the plasma membrane. J Cell Biol 2000;150:193–203.
44. Davies SP, Reddy H, Caivano M, Cohen P. Specificity and mechanism of action of some commonly used protein kinase inhibitors. Biochem J 2000;351:95–105.
45. van Golen KL, Wu ZF, Qiao XT, Bao L, Merajver SD. RhoC GTPase overexpression modulates induction of angiogenic factors in breast cells. Neoplasia 2000;2:418–25.
46. Zhou R, Cao X, Watson C, et al. Characterization of protein kinase A-mediated phosphorylation of ezrin in gastric parietal cell activation. J Biol Chem 2003;278: 35651–9.
47. Yang HS, Hinds PW. Increased ezrin expression and activation by CDK5 coincident with acquisition of the senescent phenotype. Mol Cell 2003;11:1163–76.
48. Autero M, Heiska L, Ronnstrand L, et al. Ezrin is a substrate for Lck in T cells. FEBS Lett 2003;535:82–6.
49. Wu YX, Uezato T, Fujita M. Tyrosine phosphorylation and cellular redistribution of ezrin in MDCK cells treated with pervanadate. J Cell Biochem 2000;79:311–21.
50. Vanni C, Parodi A, Mancini P, et al. Phosphorylation-independent membrane relocalization of ezrin following association with Dbl in vivo. Oncogene 2004;23: 4098–106.